First-principles lattice dynamics of almost-unstable zinc-blende structures

J. W. Kremer and K. H. Weyrich
Theoretische Physik, Universität des Saarlandes, D-6600 Saarbrücken, Federal Republic of Germany
(Received 12 June 1989)

Using a full-potential linear-muffin-tin-orbital method (LMTO-FP), *ab initio* calculations of the Γ-point phonon spectrum and elastic properties of the copper halides CuF, CuCl, CuBr, and CuI (and for purpose of comparison of Si, ZnSe, and ZnTe) were performed. Our results for the TO(Γ)-phonon frequencies, the bulk modules, and the piezoelectrically stiffened shear modules agree very well with the experimental values, establishing thus the accuracy of the LMTO-FP method. The experimental determination of the optical mode Grüneisen parameters is quite difficult, as there is a strong dependence of the structure of the Raman spectrum on the applied hydrostatic pressure. These difficulties can be totally avoided by our method, so we obtain reliable optical mode Grüneisen and internal-strain parameters. Moreover, the LMTO-FP method has been used to test the proposed Cu off-center model for CuCl, which could not be confirmed by our *ab initio* calculation.

I. INTRODUCTION

Copper halides belong to the substances with zinc-blende structure, but their Phillips ionicity is near the critical value for the transition to the rocksalt structure.[1] Therefore interesting lattice dynamical properties should be expected; and since the mid-1970s, a lot of experimental and theoretical effort has been devoted to their study. The phonon spectrum of the copper halides has been determined by inelastic neutron scattering over a broad temperature range and was fitted with various models.[2–7] At low temperatures, CuCl and CuBr show a negative thermal expansion coefficient,[8] which was related to negative mode Grüneisen parameters for the shear modules.[9] Measurements of the elastic constants[9,10] yielded unusually small c_{11}-c_{12} values.

A lot of interest has been drawn by anomalies in the Raman spectrum of CuCl (and less pronounced of CuBr and CuI). Though—due to the symmetry of the zinc-blende structure—only one transverse-optic Γ-point phonon should exist, a complex line spectrum can be observed,[11,12] of which two lines are attributed to TO(Γ) phonons. Moreover, the structure of the Raman spectra varies with temperature[13] and applied hydrostatic pressure.[14,15] As an explanation, additional off-center positions for the copper atoms were supposed, giving rise to a second TO(Γ) mode.[13,16,17] Other models propose a resonance between the bare TO(Γ) phonon and the two-phonon density of states.[7,12,15,18]

The electronic band structure of the copper halides has been calculated within the framework of the density-functional theory in the local-density approximation (DFT-LDA).[19] Results of non-self-consistent KKR calculations as well as of a self-consistent linear-muffin-tin-orbital atomic-sphere (LMTO-ASA) calculation for CuCl were compared to some measured optical properties. Since the DFT is by construction a ground-state theory, the excitonic effects could only be moderately described.

In our paper, we present *ab initio* calculations of the Γ-point phonon spectrum and elastic properties of the copper halides CuF, CuCl, CuBr, and CuI. They were done within the DFT-LDA, using a full-potential linear-muffin-tin-orbital (LMTO-FP) method. The frequencies of the transverse-optical Γ-point phonons, their volume dependence, and the corresponding mode Grüneisen parameters could be determined. As our calculations yield directly the bare TO(Γ) phonon frequency, all difficulties related to the evaluation of the Raman experiments were avoided. The proposed Cu off-center model for CuCl (Refs. 16 and 17) is reviewed critically. To describe the behavior of the acoustic-phonon branches, we determine the bulk modules, the piezoelectrically stiffened shear modules c_{44}^{D}, and the corresponding internal strains as well as their mode Grüneisen parameters.

After reviewing in Sec. II the LMTO-FP method, we present in Sec. III the results for the TO(Γ) phonon, the corresponding mode Grüneisen parameters, and deal in particular with the special situation for CuCl. The elastic properties of the copper halides are discussed in Sec. IV: we give our results for the lattice constants, the bulk modules, the internal strain related to a rhombohedral shear, the piezoelectrically stiffened shear modules, and their variations under hydrostatic pressure. Finally, a summary concludes the paper.

II. THE FULL-POTENTIAL LMTO METHOD

The theory of the LMTO-FP method has been described in full detail elsewhere.[20] Therefore we shall confine ourselves here to emphasizing its general properties, which are crucial for the validity of our results.

Most important is, that our LMTO version takes into account the full potential without any shape approximation. We use the density-functional formalism in the Kohn-Sham scheme to get a single-particle Schrödinger equation, whose solutions allow the construction of the electronic ground-state density. Using the Born-Oppenheimer approximation, the obtained Kohn-Sham

total energy represents the ground-state energy of the various forms of lattice distortions we will deal with.

Within the LMTO-FP, the effective potential V in the Schrödinger equation is described as a sum of localized parts $\hat{V}$ and a smooth pseudopart $\tilde{V}$. Denoting the position of the atoms in the primitive cell by $\mathbf{Q}$, the translation vectors of the lattice by $\mathbf{T}$ and introducing $L=(l,m)$ as angular momentum index, we can write

$$V(\mathbf{r})=\sum_{\mathbf{T}}\sum_{\mathbf{Q}}\hat{V}_{\mathbf{Q}}(\mathbf{r}-\mathbf{Q}-\mathbf{T})+\sum_{\mathbf{G}}\tilde{V}(\mathbf{G})e^{i\mathbf{G}\cdot\mathbf{r}} \quad (1)$$

where the Fourier-expanded part extends over the whole lattice. The localized part is nonzero only inside spheres around atomic sites and vanishes differentiably at the sphere boundaries. It is given by

$$\hat{V}_{\mathbf{Q}}(\mathbf{r})=\sum_{L}\hat{V}_{\mathbf{Q}L}(r)Y_L(\hat{\mathbf{r}}) . \quad (2)$$

This decomposition in spherical harmonics and Fourier series is overcomplete inside the atomic spheres, so we used in our calculations only the $L=0$ terms in (2), which means that the whole nonsphericity of the potential is described by plane waves. The Fourier expansion of $\tilde{V}$ was limited to $|\mathbf{G}|\leq 10(2\pi/a)$ (with a denoting the lattice constant), thus retaining 1067 coefficients.

The solutions of the Schrödinger equation are expressed in a LMTO basis set, whose basis functions are Bloch functions, consisting inside the atomic spheres of solutions to the spherically symmetrized potential. At the sphere boundaries, they match continuously and differentiably to solutions of the Laplace equation. It is this property which forces all our solutions constructed from the LMTO basis to have zero kinetic energy in the interstitial region. As we shall see, this restriction seems not to influence the accuracy of the results presented below, which has partly been stated earlier.[21]

To reduce the interstitial space in the zinc-blende structure, in addition to the Cu atom at the origin of the elementary cell and the halide atom near $(\frac{1}{4},\frac{1}{4},\frac{1}{4})a$, two empty spheres were inserted at $(\frac{1}{2},\frac{1}{2},\frac{1}{2})a$ and $(\frac{3}{4},\frac{3}{4},\frac{3}{4})a$. The common radius of all four MT spheres was chosen in such a way that no overlap occurred, even in distorted configurations, resulting in a space filling of 59.4%.

The employed LMTO basis consisted of s, p, and d orbitals at each atomic and empty site, giving a total of 36 basis functions. For a better representation of the band structure, we used two panels to linearize the energy dependence of the wave functions. The lower one contained the halide s orbital, whereas its p and the copper d electrons were in the upper panel. All other electrons have been taken into account by a frozen atomic core, renormalized to the MT sphere.

Copper fluoride, which has the smallest Cu MT radius, has been used to test the influence of the core size and the effect of the core renormalization. We included in addition the Cu $3p$ electrons in the band calculation, without seeing any remarkable change in the relative energies.

Integrations over the Brillouin zone were performed using the method of special $\mathbf{k}$ points;[22,23] depending on the symmetry of the lattice, we took one to three $\mathbf{k}$ points. Test calculations with a larger set of $\mathbf{k}$ points gave no improvements of the relevant total-energy differences.

Starting with a potential of the form (1), we calculate solutions of the DFT-Schrödinger equation and express them as sums of localized parts and a pseudowave function. Summing up over all occupied orbitals, a new nonspherical density is calculated and—in the frame of the LDA—a new potential is constructed. This cycle is iterated until self-consistency is achieved, i.e., the total energy is converged.

III. THE TO(Γ) PHONON

A. Frozen-phonon calculation

To determine the frequency of the TO(Γ) phonon, we proceeded as in Refs. 20 and 21. The origins of the fcc Cu and halide sublattices were placed at

$$(0,0,0) \text{ and } (1+\gamma)(\tfrac{1}{4},\tfrac{1}{4},\tfrac{1}{4})a , \quad (3)$$

respectively, and the LMTO-FP total energy for these configurations has been calculated. To account for the phonon anharmonicity, positive as well as negative values for γ were chosen; in most calculations we used $\gamma=\pm 0.02$. The resulting total-energy differences between the distorted and the undistorted configuration were typically of the order of 3 meV, corresponding to a temperature of some 30 K. This indicates that the applied phonon amplitudes are of reasonable order to compare our results with experiments carried out at low temperatures.

Expanding the total-energy increase ΔE in a Taylor series with respect to the phonon amplitude u, we obtain

$$\Delta E=A\left[\frac{u}{a}\right]^2+B\left[\frac{u}{a}\right]^3 =A\left[\frac{u}{a}\right]^2\left[1+\frac{B}{A}\left[\frac{u}{a}\right]\right] \quad (4)$$

and with the reduced mass μ, the phonon frequency ν_{TO} is given by

$$\nu_{\mathrm{TO}}=\frac{1}{2\pi a}\sqrt{A/2\mu} . \quad (5)$$

Equation (5) shows that the relative errors in the phonon frequency are only about half as large as those in the total-energy differences.

Our results for A, B, B/A, and the calculated as well as the experimental phonon frequencies are given in Table I for the four copper halides and in addition for Si, ZnSe, and ZnTe. With the exception of the special situation for CuCl, which will be discussed in detail below, the agreement between the calculated ν_{TO} and the experimental values is excellent. This indicates that the LMTO-FP method yields reliable results not only for group-IV and III-V semiconductors as already shown before, but also for transition-metal compounds. It should be emphasized that—in contrast to methods using a plane-wave basis set—our calculations for the copper halides require essentially the same computational effort as those for silicon.

TABLE I. Calculated second- and third-order coefficients A and B (in keV) as well as the degree of anharmonicity B/A of the potential for a TO(Γ)-phonon distortion. The calculated and experimental phonon frequencies ν_{TO} are given in THz. The slight differences to the values given in Ref. 21 result from an improved total-energy convergency.

	A	B	$\frac{B}{A}$	ν_{TO}	ν_{TO}(expt.)
Si	0.8214	−7.88	−9.6	15.57	15.46[a]
ZnSe	0.3944	−5.949	−15.1	6.49	6.39[a]
ZnTe	0.4245	−6.368	−15.0	5.69	5.31[a]
CuF	0.401	−9.55	−23.8	13.59	
CuCl	0.1194	−3.10	−26.0	4.68	4.47 (β)[b]
					5.19 (γ)[b]
CuBr	0.1564	−3.60	−23.0	4.08	4.08[a]
					4.20[b]
CuJ	0.2162	−4.86	−22.5	4.14	3.99[b]
					4.02[a]

[a]Reference 8.
[b]Reference 13.

B. The TO(Γ) phonon in CuCl

For a harmonic crystal with zinc-blende structure, group theory predicts only one TO(Γ) phonon, whereas in CuCl a complex line spectrum has been observed with ir, Raman, and neutron scattering experiments[5,12–15] (for further references see, e.g., Ref. 7). Two lines of this spectrum, labeled β and γ, are considered to be TO phonons. Several models have been developed to explain this phenomenon.

Vardeny and Brafman[16] supposed that there are four equivalent off-center minima for the copper position. They should be displaced from the ideal sites in a direction parallel to one of the cube diagonals toward the "holes" in the zinc-blende structure, i.e., versus our empty sphere positions. The potential curvature at the ideal sites should determine the γ lines, whereas the β peaks arise from the off-center positions. In a later paper,[17] there was also proposed an explicit potential function for the Cu elongation.

Our calculated TO(Γ) frequency of 4.68 THz is far away from the γ line at 5.19 THz. Moreover, for such a potential with several minima, a strong anharmonicity should be expected. The B/A values in Table I quantify the correction to the harmonic potential by third-order terms. An increasing anharmonicity can be seen from silicon over ZnSe, ZnTe to the copper halides. Though B/A for CuCl is slightly higher than for the other copper halides, this difference seems not to be significant enough to justify the proposed potential.

To further investigate this problem, we calculated the total energy for a series of Cu sublattice displacements in the direction of the supposed off-center minimum. These configurations correspond to a collective movement of all copper atoms, neglecting the fact that different Cu atoms could occupy different minima. This simplification had to be made, to maintain lattice periodicity. Nevertheless, this scenario should be covered exactly by the model in Ref. 17, where neither a relaxation of the Cl sublattice nor a possible correlation of the positions of neighboring Cu atoms has been considered.

We calculated the Cu displacement potential for Cu positions described by γ values [Eq. (3)] of up to 0.23, i.e., with amplitudes more than ten times as large as used for the frozen-phonon calculations. To avoid any overlap it was necessary to shrink the radius of the MT spheres used in all other calculations and thus to reduce the space filling by about 2%. As a test, we repeated the TO(Γ)-phonon frequency calculation with the smaller MT spheres, obtaining nearly exactly the same result as above.

Over the whole range, our calculated displacement potential (Fig. 1) can be satisfactorily approximated by a polynomial with second-, third-, and fourth-order terms, as indicated by the solid line in Fig. 1. For a comparison, we have also depicted the potential given in Ref. 17. Obviously, in our *ab initio* potential there is no evidence at

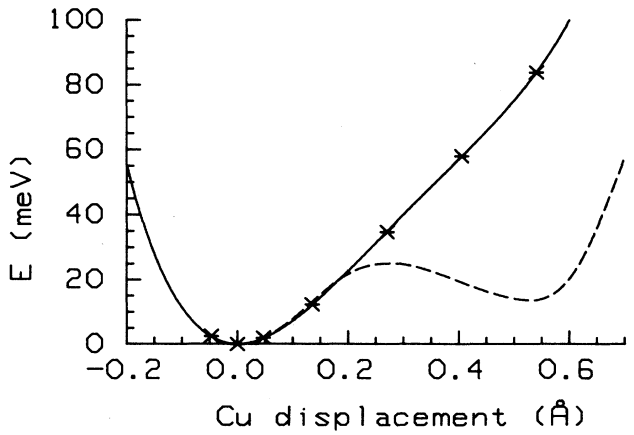

FIG. 1. Off-center displacement potential for CuCl. Our calculated values are indicated by asterisks, the solid line represents a fit with a fourth-order polynomial. For comparison, the proposed potential of Ref. 17 is also shown (dashed line).

all for an off-center minimum, so we believe that this model can be ruled out.

Another model to explain the Raman spectrum of CuCl was given by Krauzman *et al.*[12] They proposed a resonance between the TO(Γ)-phonon and the two-phonon density of states. Fitting their model to the measured line shapes, they derived the frequency of the bare TO(Γ) phonon to be 158 $cm^{-1} \cong 4.74$ THz, which is in excellent agreement with our calculated value of 4.68 THz.

Recently, this model has been refined by calculating the Raman and neutron spectra in the frame of a valence-shell model.[7] Kanellis *et al.*[18] could explain the TO(Γ)-phonon line shapes for CuCl, CuBr, and CuI, taking into account the leading third-order anharmonic coupling terms.

C. Mode Grüneisen parameter

The frozen-phonon calculations described in Sec. III A were repeated for different lattice constants. This gives the dependence of the TO(Γ)-phonon frequency ν from the unit cell volume V. Therefrom, the mode Grüneisen parameters γ_i can be obtained directly via

$$\gamma_i = -\frac{\partial(\ln \nu_i)}{\partial(\ln V)} = -\frac{V}{\nu_i}\frac{\partial \nu_i}{\partial V} \ . \tag{6}$$

To keep the required numerical effort in reasonable limits, in most cases we calculated ν_{TO} for three different lattice constants: the experimental value, a compressed, and an expanded configuration. With each pair of frequencies, the derivatives in (6) can be approximated by two-point formulas:

$$\gamma_i \approx \gamma_i^* = -\frac{\ln(\nu/\nu')}{\ln(V/V')} \tag{7}$$

or

$$\gamma_i \approx \gamma_i^{**} = -\frac{1-\nu'/\nu}{1-V'/V} \ . \tag{8}$$

In most cases, the γ_i^* and γ_i^{**} were quite different, so we had to use all three ν_{TO} values to apply a three-point derivative formula.

Our results for the mode Grüneisen parameters are shown in Table II. An estimation of the technical errors, introduced by the not fully converged total energy and the discretization of the derivative, is also given.

In the case of Si, ZnSe, and ZnTe, the agreement of our values with the experimental results is very good. The calculation by Nielsen and Martin[24] has been done by an *ab initio* pseudopotential method; all the model calculations mentioned in Table II contain parameters, which were fitted to experimental data.

For the copper halides, the experimental values of the Grüneisen parameter were obtained from Raman scattering measurements under hydrostatic pressure.[14,15] The TO(Γ) peak in CuI and—for low temperatures—in CuBr, can be determined unambiguously. But for CuCl, there is a complex Raman spectrum, and the determination of ν_{TO} depends on the fit to a model, as discussed in Sec. III B. Moreover, these experiments give only the pressure derivative $\partial\nu/\partial p$, which has to be transformed via the bulk modulus into the required volume derivative. This introduces additional uncertainties due to the temperature and pressure dependence of the bulk modulus, as discussed below in Sec. IV A.

With this background, we understand the reasonable agreement of our results for CuI and CuBr with the experiments and the larger discrepancy for the CuCl value. As we obtain from our calculations the frequency of the bare TO(Γ) phonon without any additional model assumptions and we do not have to use other material parameters, our results should be more reliable. Further support for our higher γ_{TO} comes from a recently performed independent valence-shell-model calculation.[25]

IV. ELASTIC PROPERTIES

As is widely known, the linear-muffin-tin-orbital method (LMTO) in atomic-sphere approximation[26] (ASA) yields accurate band structures, lattice constants, and bulk modules. Ves *et al.*[19] applied this method to

TABLE II. Calculated and experimental TO(Γ)-phonon mode Grüneisen parameters $\gamma_{TO(\Gamma)}$ together with results from other *ab initio* and model calculations. For our calculations, the technical errors are indicated.

	$\gamma_{TO(\Gamma)}$	$\gamma_{TO(\Gamma)}$(expt.)	Other calc.	Model calc.
Si	0.94±0.01	0.98±0.06[a]	0.9[b]	1.06[a]
ZnSe	1.55±0.01	1.4[c]		1.22[d]
ZnTe	1.50±0.02	1.7[c]		1.5[a]
		1.6±0.1[a]		1.4[d]
CuCl	3.2±0.25	2.4[e]		3.4[f]
CuBr	2.8±0.15	2.4[g]		
CuJ	2.5±0.25	2.2[g]		

[a]B. A. Weinstein and G. J. Piermarini, Phys. Rev. B **12**, 1172 (1975), and references therein.
[b]Reference 24.
[c]M. Cardona, J. Phys. (Paris) Colloq. **45**, C8-29 (1984).
[d]D. N. Talwar, M. Vandevyver, K. Kunc, and M. Zigone, Phys. Rev. B **24**, 741 (1981).
[e]Reference 15.
[f]Reference 25.
[g]Reference 14.

compute electronic band structures for copper halides in the zinc-blende and the high-pressure rocksalt phase. Simulating the effect of hydrostatic pressure by varying the lattice constant, they obtained reasonable results for the deformation potential.

On the other hand, experience shows that the LMTO-ASA method yields decreasing energy variations, if nonhydrostatic pressures or phonon distortions are applied. This is an effect of the spheroidization of the charge density inside overlapping spheres and the resulting errors in the Hartree part of the total-energy functional. If the spheroidization of the charge density is avoided, this unphysical instability is removed, but due to the still spherical potential, the calculated shear constants and phonon frequencies are too high.

Accurate shear constants and phonon frequencies are obtained, if also the nonspherical part of the potential is taken into account and the spheres are not overlapping.[20,21,27] Performing these calculations, we have to take special care to avoid volume changing distortions. The reason lies in the incompleteness of our LMTO basis set in the interstitial region: if, e.g., the volume is compressed, either the MT spheres shrink proportionally, with the effect that more charge lies in the less accurately represented interstitial region, or the space filling ratio of the MT spheres has to be changed. In the former case, we have a tendency to higher energies at small volumes, in the latter, the effect is inverse. As its magnitude cannot be estimated in advance, the only way to eliminate it is to keep the volume—and thus the basis set—constant.

A. Lattice constant and bulk modulus

We normally use the LMTO-ASA method to produce a start potential for our LMTO-FP self-consistency iteration cycle. As a byproduct, it was easy to obtain theoretical lattice constants and bulk modules. To that purpose, we calculated self-consistent LMTO-ASA ground-state energies $E_{\rm tot}$ for various lattice volumes around the experimental value. The equilibrium lattice volume is given by the zero of the applied hydrostatic pressure $p(V)$, with

$$p(V)=-\frac{dE_{\rm tot}}{dV} . \tag{9}$$

It turned out that it was sufficient to have the ground-state energy for a few values of V, approximate the function $E_{\rm tot}(V)$ by a polynomial of third or fourth degree, and to determine its minimum. The resulting lattice constants are given in Table III together with the experimental values. All results have an error of less than 1.2%, which is quite common for the ASA method and contributed mostly to the local-density approximation.

The adiabatic bulk modulus B_T is given by

$$B_T=-V\frac{dp}{dV}=V\frac{d^2E_{\rm tot}}{dV^2} . \tag{10}$$

Again, the derivative was calculated from an approximating polynomial; but to get consistent results, higher-order polynomials, i.e., more points $E_{\rm tot}(V)$ needed to be taken into account.

We have an excellent agreement of our CuCl result with the bulk modulus gained from inelastic neutron scattering at 4.5 K.[4] For further comparisons we have only experiments at significantly higher temperatures at hand (see Fig. 2). Ultrasonic measurements at 300 K gave bulk modules, which are as much as some 40% (CuCl) and some 25% (CuBr, CuI) smaller than our results. Also a result from inelastic neutron scattering at 77 K yielded a 19% smaller $B_{\rm expt}$ for CuBr.

This strong temperature dependence of some of the elastic constants has already been discussed in Ref. 4, where it has been attributed to the strong anharmonicity of the Cu potential. In Secs. III A and III B we examined the potential of the TO(Γ)-phonon elongation and found a relatively large anharmonicity common to the copper halides. Moreover, we can understand from our B/A values (Table I), that the temperature dependence of the bulk modulus should be strongest in the case of CuCl.

In the same manner as described above, we also obtained values for the pressure dependence dB/dp of the bulk modulus

$$\frac{dB}{dp}=-\left[1+V\frac{d^3E}{dV^3}\left[\frac{d^2E}{dV^2}\right]^{-1}\right] . \tag{11}$$

With the exception of CuBr, these values are considerably larger than, e.g., for Si, where a value of 4.15 has been measured.

B. Calculation of shear modules

The calculation of elastic constants is in principle straightforward: for a suitable chosen strain tensor $\underline{\epsilon}$, the

TABLE III. Lattice constants a (in Å) and bulk modules B (in Mbar), calculated with the LMTO-ASA method and experimental values. The calculated pressure dependence dB/dp is given in the last column.

	$a_{\rm ASA}$	$a_{\rm expt}$	$B_{\rm ASA}$	$B_{\rm expt}$	$\frac{dB_{\rm ASA}}{dp}$
CuCl	5.35	5.41[a]	0.66	0.654 [4.5 K][b] 0.38 [300 K][c]	6.2
CuBr	5.63	5.69[a]	0.54	0.436 [77 K][c] 0.39 [300 K][c]	3.7
CuI	6.01	6.04[a]	0.48	0.355 [300 K][c]	8.0

[a]Reference 8.
[b]Reference 3.
[c]Reference 10.

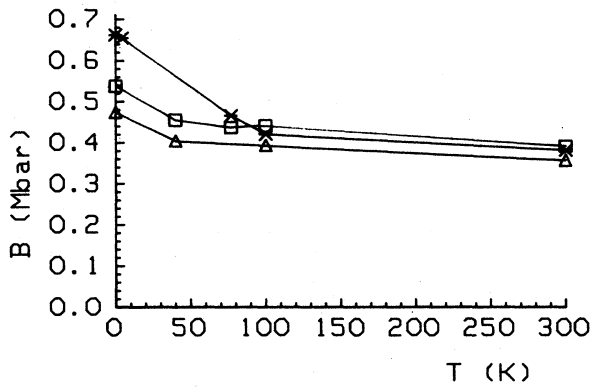

FIG. 2. Temperature dependence of the bulk modulus for CuCl (*), CuBr (□), and CuI (△). Values for $T=0$ are calculated, others taken from elastic constants in Ref. 8. Straight lines connect the points belonging to the same material.

ground-state energies of a strained and an unstrained crystal configuration are determined. The desired combination of elastic constants is now directly related to the difference of the ground-state energies and the elements of $\underline{\epsilon}$.

Proceeding as just outlined, some technical as well as physical peculiarities have to be taken into account. One of them is, that, as already discussed, we have to restrict $\underline{\epsilon}$ to volume conserving strains, so we need

$$\det(\underline{1}+\underline{\epsilon})=1 \ . \tag{12}$$

Another crucial point is the choice of the reciprocal lattice points used to represent the Fourier-expanded parts of the potential [Eq. (1)], wave functions, and electron density. Reliable total-energy differences can only be obtained if the set of **G** vectors in the strained and unstrained configuration remains, apart from the distortion, identical; similar observations have also been made for pseudopotential calculations.[24] So we use the cutoff procedure given in Sec. II only once and then strain the **G** mesh.

For the calculation of c_{44}, a strain of the form

$$\underline{\epsilon}=\begin{pmatrix} e_1 & \frac{1}{2}e_6 & \frac{1}{2}e_5 \\ \frac{1}{2}e_6 & e_2 & \frac{1}{2}e_4 \\ \frac{1}{2}e_5 & \frac{1}{2}e_4 & e_3 \end{pmatrix} \tag{13}$$

with

$$e_1=e_2=e_3=:e'; \quad e_4=e_5=e_6=:e \tag{14}$$

proved to be favorable. It corresponds to a stress, stretching the cubic elementary cell in the direction of the [111] space diagonal, producing a rhombohedral strain.

The volume conservation (12) yields

$$e'=\tfrac{1}{4}e^2+O(e^3) \ . \tag{15}$$

This formula serves to evaluate the elastic energy, whereas for the determination of the distorted crystal configuration, we use the exact value of e', to have the best possible volume conservation.

Expressing the deformation energy ΔE of a lattice with volume V in the framework linear elasticity theory yields

$$U=\frac{\Delta E}{V}=\tfrac{1}{2}\mathbf{e}^T\underline{C}\mathbf{e}=\tfrac{3}{2}c_{44}e^2+\tfrac{9}{32}Be^4+O(e^5) \ . \tag{16}$$

The terms of order e^4 and higher in (16) can safely be neglected, as the bulk modulus B is roughly of the same magnitude as c_{44}, and we always choose $e\leq 0.02$. Then the shear modulus c_{44} can be obtained via

$$c_{44}\approx\frac{2\Delta E}{3V}\frac{1}{e^2} \ . \tag{17}$$

Comparing this result with (4) and (5) we see that the relative error in the elastic constants is of the same order as for the total-energy difference ΔE and not only about the half, as for ν_{TO}. It is mainly due to that reason, we have to take into account the relative minor technical effects discussed above.

C. Internal strain and piezoelectrically stiffened shear modulus

Applying the rhombohedral strain discussed above to the zinc-blende structure, the position of the atom near $(1,1,1)a/4$ is no longer fully determined by symmetry, as it is in the normal configuration, where this atom lies exactly in the center of the tetrahedron, formed by the four neighboring Cu atoms. There is an additional degree of freedom in the [111] direction, the internal strain ξ. The position of the halide atom can now be described by

$$[1+(1-\xi)(e'+e)](1,1,1)\frac{a}{4} \ . \tag{18}$$

If the parameter ξ is zero, the atom follows completely the applied strain, whereas $\xi=1$ corresponds to the situation where the Cu-halide bond in the direction of the space diagonal remains unchanged. Normally, one would expect ξ to be anywhere in this interval; for silicon, experiments and calculations yielded $\xi\approx 0.5$.[24]

To obtain the parameter ξ, we made for each material three complete total-energy calculations for the rhombohedrally distorted configuration, using the internal strains $\xi=0.0, 0.5, 1.0$. Then, ξ was determined as the minimum of the total energy with respect to the internal strain; the applied procedure was similar to the one discussed above for the lattice constants. The energies in the different runs were typically less than 1 meV apart, which gives rise to possible uncertainties in ξ, whereas the value for the energy minimum is quite stable. Comparing it with the energy in the unstrained case yields the distortion energy ΔE, and finally c_{44} [Eqs. (16) and (17)].

For piezoelectric semiconductors with zinc-blende structure, two different shear constants, namely c_{44}^E and the piezoelectrically stiffened constant c_{44}^D can be measured.[28] The frequency of a transverse-acoustic phonon propagating along one of the cubic axes is determined by c_{44}^E, whereas an acoustic phonon in the [011] direction with polarization along [100] gives rise to a piezoelectric effect, and thus sees c_{44}^D.

Our rhombohedral strain corresponds to the long-

wavelength limit ($\mathbf{k}\to 0, \mathbf{u}\cdot\mathbf{k}=\text{const}$) of a superposition of three phonons of the latter type. By writing for the resulting elongation $\mathbf{u}$

$$u_1(\mathbf{R},t)=u\sin[k(R_2+R_3)-\Omega t]$$
$$\underset{\mathbf{k}\to 0}{\to} u\sin(-\Omega t)+uk(R_2+R_3)\cos(\Omega t)+O(k^2) \tag{19}$$

and cyclically for u_2 and u_3, respectively, we can calculate the elements of the strain $\mathbf{e}$ to be

$$e_1=2\frac{\partial u_1}{\partial R_1}=0\ , \tag{20}$$

$$e_4=\frac{\partial u_2}{\partial R_3}+\frac{\partial u_3}{\partial R_2}$$
$$=uk\{\cos[k(R_1+R_3)-\Omega t]+\cos[k(R_1+R_2)-\Omega t]\}$$
$$\underset{\mathbf{k}\to 0}{\to} 2uk\cos(\Omega t)+O(k^2) \tag{21}$$

and analogously for the other components of $\mathbf{e}$.

Identifying e in (14) with the term $2uk\cos(\Omega t)$ in (21), we see that we have the same strain tensor, if the small diagonal elements e' [Eq. (15)], coming from the volume conservation, are neglected. Also, the homogeneous distortion $\mathbf{u}$ resulting from the strain [Eq. (13)]

$$\mathbf{u}=\underline{\epsilon}\mathbf{R}+\mathbf{u}_0=\tfrac{1}{2}e\begin{bmatrix}R_2+R_3\\R_1+R_3\\R_1+R_2\end{bmatrix}+\mathbf{u}_0 \tag{22}$$

can be identified with the limit in Eq. (19).

The results at the experimental lattice constant for the internal strain parameter ξ and the elastic constant c_{44}^D are shown in Table IV together with experimental results. Our elastic constants differ by only about 1% from the measured quantities. The internal strain, where no experimental data seem to be available, lies in the expected range and shows a pronounced tendency to higher values with increasing ionicity.

D. Rhombohedral shear under hydrostatic pressure

We repeated the internal strain calculations and the determination of c_{44}^D for the copper halides under hydrostatic pressure. To get the volume dependence of these variables requires a considerable numerical effort, as for each lattice volume four independent self-consistent full-potential runs had to be made. Therefore we treated only three to five different lattice constants for each material, which turned out to be sufficient to elucidate the physical behavior.

TABLE IV. Internal strain parameter ξ and piezoelectrically stiffened shear constant c_{44}^D (in Mbar).

	ξ	c_{44}^D	c_{44}^D(expt)
CuCl	0.57	0.162	0.1635[a]
CuBr	0.45	0.151	0.1492[b]
CuI	0.40	0.187	0.1852[b]

[a]Reference 4.
[b]Reference 10.

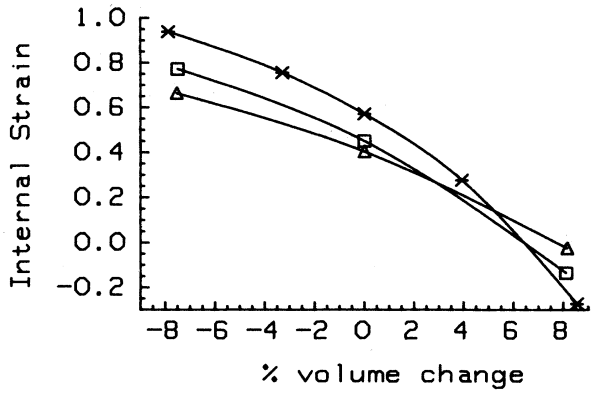

FIG. 3. Calculated internal strain parameter ξ of CuCl (*), CuBr (□), and CuI (△) as function of the relative volume change. The solid curves only serve as a guide to the eye.

In Fig. 3, the internal strain in relation to the relative volume change is depicted. We state a similar behavior for all three copper halides; with increasing lattice volume the internal strain decreases monotonically. The physical interpretation is, that the more the lattice is compressed, the more there is a tendency to keep the length of the [111] copper-halide bond constant, when the strain (13), (14) is applied.[29] In contrary, if the lattice is blown up by more than about 5%, the ions follow closely the applied strain, expressed through $\xi\approx 0$; the slightly negative values for ξ we got in our calculations can be attributed mainly to extrapolation errors.

Evaluation of our results for the volume dependence of c_{44}^D (Fig. 4) shows up a different behavior of the three materials in question. In the case of CuI, we see an approximately linear dependence. Determination of the corresponding mode Grüneisen parameter, which is given by

$$\gamma_{c_{44}^D}=-\frac{1}{6}-\frac{1}{2}\frac{\partial\ln(c_{44}^D)}{\partial\ln(V)} \tag{23}$$

yielded a value of 1.7, which is larger than the experimental c_{44} Grüneisen parameters for other materials, as cited e.g. in Ref. 9.

For CuBr, the situation is characterized by a

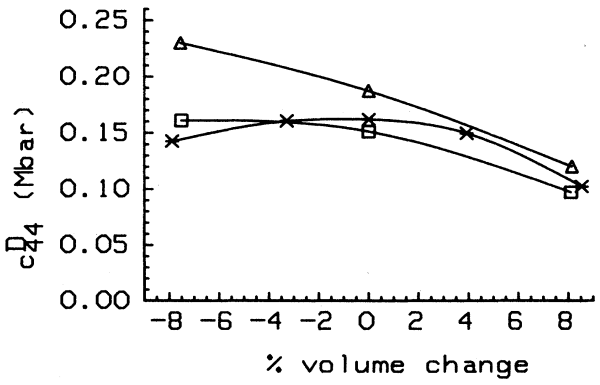

FIG. 4. Calculated shear modulus c_{44}^D of CuCl (*), CuBr (□), and CuI (△) as function of the relative volume change. The solid curves only serve as a guide to the eye.

significant flattening of the volume dependence of c_{44}^D, when the lattice is compressed. Equation (23) was evaluated by a polynomial fit to our calculated c_{44}^D values with a procedure similar to the one described in Sec. III C. This yields a Grüneisen parameter of about 1.2.

The nonlinear behavior of c_{44}^D was strongest for CuCl, in agreement with experiments,[9] which observed a significant second-order term. From our results, we get a maximum of c_{44}^D for a lattice constant corresponding nearly to the zero-pressure volume V_{expt}. So, our mode Grüneisen parameter is very close to zero, when Eq. (23) is evaluated at V_{expt}. But we can clearly see that c_{44}^D decreases under hydrostatic pressure, leading to a negative mode Grüneisen parameter, as it has been measured.[9] This contributes, together with the negative mode Grüneisen parameters for c_{44}^E and $c_{11}-c_{22}$, to the negative thermal expansion coefficient of CuCl at low temperatures.

V. SUMMARY

In this paper, the recently developed LMTO-FP method has been applied to transition-metal compounds. The TO(Γ) phonon frequencies we obtained for Si, ZnSe, ZnTe, CuBr, and CuI agree very well with the measured values. In the case of CuCl with its double TO(Γ) line in the Raman spectrum, our calculated frequency matches the bare phonon frequency derived from a one-phonon–two-phonon interaction model.[12] For the Cu off-center model,[16] which has been proposed as an alternative, we recalculated *ab initio* the suggested displacement potential,[17] but could not confirm the predicted double minimum structure.

By varying the lattice constant in our calculations, we determined directly the mode Grüneisen parameters for the TO(Γ) phonon. For Si, ZnSe, and ZnTe, the results are within the error margins of the available experimental data. Our mode Grüneisen parameters for the copper halides are without exception larger than the given measured values, showing up the greatest discrepancy for CuCl. Due to the experimental difficulties discussed above, we believe that our values are more reliable, which is also confirmed by a model calculation of γ_{TO} for CuCl.[25]

With LMTO-ASA calculations, we could determine the lattice constants of all copper halides as well as the $T=0$ bulk modulus of CuCl with an accuracy of about 1%. For CuBr and CuI, where no low-temperature measurements of the bulk modulus seem to be available, we predict a stiffening of this elastic constant, as is the case for CuCl.

Applying a rhombohedral shear, we calculated the elastic constants c_{44}^D, differing by less than 1.2% from the measured values. The dependence of the internal strain parameter and of c_{44}^D from an additional hydrostatic pressure has been determined.

With the preceding results, we have shown that the LMTO-FP method can be successfully applied not only to materials which have covalent bonds, but also to the more ionic transition-metal compounds. We obtained accurate results, which reproduced very well the experimental data. Moreover, properties whose measurement is difficult or nearly impossible could be reliably calculated.

ACKNOWLEDGMENTS

We gratefully acknowledge the helpful advice of O. K. Andersen and R. Siems. This work was partially supported by the Deutsche Forschungsgemeinschaft within the framework of the Sonderforschungsbereich 130.

[1] J. C. Phillips, Rev. Mod. Phys. **42**, 317 (1970).
[2] B. Prevot, C. Carabatos, C. Schwab, B. Hennion, and F. Moussa, Solid State Commun. **13**, 1725 (1973).
[3] S. Hoshino, Y. Fujii, J. Harada, and J. D. Axe, J. Phys. Soc. Jpn. **41**, 965 (1976).
[4] B. Prevot, B. Hennion, and B. Dorner, J. Phys. C **10**, 3999 (1977).
[5] B. Hennion, B. Prevot, M. Krauzman, R. M. Pick, and B. Dorner, J. Phys. C **12**, 1609 (1979).
[6] M. S. Kushwaha, Can. J. Phys. **60**, 1589 (1982).
[7] G. Kanellis, W. Kress, and H. Bilz, Phys. Rev. B **33**, 8724 (1986).
[8] *Numerical Data and Functional Relationships in Science and Technology, New Series III,* Vol. 17 of *Landolt-Börnstein,* edited by O. Madelung, M. Schulz, and H. Weiss (Springer, Berlin, 1982); *Numerical Data and Functional Relationships in Science and Technology, New Series III,* Vol. 22a of *Landolt-Börnstein,* edited by O. Madelung, M. Schulz, and H. Weiss (Springer, Berlin, 1982).
[9] R. C. Hanson, K. Helliwell, and C. Schwab, Phys. Rev. B **9**, 2649 (1974).
[10] R. C. Hanson, J. R. Hallberg, and C. Schwab, Appl. Phys. Lett. **21**, 490 (1972).
[11] J. E. Potts, R. C. Hanson, C. T. Walker, and C. Schwab, Solid State Commun. **13**, 389 (1973).
[12] M. Krauzman, R. M. Pick, H. Poulet, G. Hamel, and B. Prevot, Phys. Rev. Lett. **33**, 528 (1974).
[13] Z. Vardeny and O. Brafman, Phys. Rev. B **21**, 2585 (1980).
[14] H. D. Hochheimer, M. L. Shand, J. E. Potts, R. C. Hanson, and C. T. Walker, Phys. Rev. B **14**, 4630 (1976).
[15] M. L. Shand, H. D. Hochheimer, M. Krauzman, J. E. Potts, R. C. Hanson, and C. T. Walker, Phys. Rev. B **14**, 4637 (1976).
[16] Z. Vardeny and O. Brafman, Phys. Rev. B **19**, 3276 (1979).
[17] G. Livescu and O. Brafman, Phys. Rev. B **34**, 4255 (1986).
[18] G. Kanellis, W. Kress, and H. Bliz, Phys. Rev. B **33**, 8733 (1986).
[19] S. Ves, D. Glötzel, M. Cardona, and H. Overhof, Phys. Rev. B **24**, 3073 (1981).
[20] K. H. Weyrich, Phys. Rev. B **37**, 10 269 (1988).
[21] K. H. Weyrich, L. Brey, and N. E. Christensen, Phys. Rev. B **38**, 1392 (1988).

[22]A. Baldereschi, Phys. Rev. B **7**, 5212 (1973).
[23]D. J. Chadi and M. L. Cohen, Phys. Rev. B **8**, 5747 (1973).
[24]O. H. Nielsen and R. M. Martin, Phys. Rev. B **32**, 3792 (1985).
[25]G. Kanellis and W. Kress (private communication).
[26]H. L. Skriver, *The LMTO Method* (Springer, Berlin, 1984).
[27]M. Methfessel, Phys. Rev. B **38**, 1537 (1988).
[28]A. R. Hutson and D. L. White, J. Appl. Phys. **33**, 40 (1962).
[29]LCAO-MO calculations for embedded molecular clusters, performed recently for CuCl and CuBr, show also $\xi \approx 1$ if the lattice volume is compressed by about 9% (CuCl) and 15% (CuBr); M. R. Press and D. E. Ellis, Phys. Rev. B **38**, 3102 (1988).